https://doi.org/10.5607/en20043
Exp Neurobiol. 2020 Oct;29(5):344-355.
pISSN 1226-2560 • eISSN 2093-8144

Original Article

Experimental Neurobiology

Distribution of K_v3 Subunits in Cochlear Afferent and Efferent Nerve Fibers Implies Distinct Role in Auditory Processing

Woo Bin Kim, Kwon-Woo Kang, Kushal Sharma† and Eunyoung Yi*
College of Pharmacy and Natural Medicine Research Institute, Mokpo National University, Muan 58554, Korea

K_v3 family K^+ channels, by ensuring speedy repolarization of action potential, enable rapid and high frequency neuronal firing and high precision temporal coding of auditory information in various auditory synapses in the brain. Expression of different K_v3 subtypes within the auditory end organ has been reported. Yet, their precise role at the hair cell synaptic transmission has not been fully elucidated. Using immunolabeling and confocal microscopy we examined the expression pattern of different K_v3 family K^+ channel subunits in the nerve fibers innervating the cochlear hair cells. $K_v3.1b$ was found in NKA-positive type 1 afferent fibers, exhibiting high signal intensity at the cell body, the unmyelinated dendritic segment, first heminode and nodes of Ranvier. $K_v3.3$ signal was detected in the cell body and the unmyelinated dendritic segment of NKA-positive type 1 afferent fibers but not in peripherin-positive type 2 afferent. $K_v3.4$ was found in ChAT-positive LOC and MOC efferent fibers as well as peripherin-positive type 2 afferent fibers. Such segregated expression pattern implies that each K_v3 subunits participate in different auditory tasks, for example, $K_v3.1b$ and $K_v3.3$ in ascending signaling while $K_v3.4$ in feedback upon loud noise exposure.

Key words: $K_v3.1b$, $K_v3.3$, $K_v3.4$, Cochlea

INTRODUCTION

K_v3 channels are high-voltage-activating type of K^+ channels that are highly expressed in neurons with high frequency firing capability [1, 2]. One important feature distinguishing K_v3 from other voltage activating K^+ channels is the rapid activation and deactivation in response to voltage changes. Such kinetic property of K_v3 enables rapid action potential (AP) repolarization while keeping the relative refractory period minimal. There are 4 members in K_v3 family: $K_v3.1$, $K_v3.2$, $K_v3.3$, and $K_v3.4$. Each member, apart from being regulated by different sets of kinases and signaling molecules, possess different inactivation properties. $K_v3.1$ and $K_v3.2$ exhibit little inactivation upon prolonged depolarization. In contrast, $K_v3.3$ and $K_v3.4$ show partial or rapid and near complete inactivation at membrane potential more positive to +10 mV, respectively.

Auditory neurons are well known for their capability of firing brief APs with high frequency and thus, able to faithfully follow the temporal pattern of high frequency inputs [3-5]. Not surprisingly, many auditory neurons express high level of K_v3 channels [6, 7]. Genetic or pharmacological manipulation of K_v3 channels in these neurons have significant impact on the firing pattern and ultimately the auditory function. *In vitro* studies have demonstrated that K^+ channel inhibitor such as TEA reduced the MNTB neuron's ability to follow high frequency neural input [8] and disturbed spike-timing in dorsal cochlear nucleus neurons [9]. Similarly, MNTB neurons from $K_v3.1$-null mice failed to fire high frequency APs [10]. $K_v3.1$-null mice exhibited attenuated acoustic startle response [11].

The widespread expression and *in vitro* impact of K_v3 channels in various auditory neurons has lead many to consider K_v3

Submitted September 10, 2020, Revised October 14, 2020,
Accepted October 16, 2020

*To whom correspondence should be addressed.
TEL: 82-61-450-2683, FAX: 82-61-450-2689
e-mail: eunyoungyi@mokpo.ac.kr
†Current affiliation: Department of Physiology and Cell Biology, School of Medicine, University of Nevada, Reno, Manville Health Science Building 1664 North Virginia Street MS0352 Reno, NV 89557 USA

as a potential therapeutic target for hearing deficit. In drug- or noise-induced hearing deficit animals, central auditory neurons often exhibited increased spontaneous firing rate [12-14] and K_v3 modulator suppressed the hearing deficit-associated hyperactivity. AUT00063, a K_v3 modulator causing leftward shift in voltage dependence and slowing deactivation speed, suppressed the hyperactivity in inferior colliculus neurons [15] and dorsal cochlear nucleus neurons [16] in noise-induced tinnitus animal. In addition, K_v3 modulator alleviated temporal processing deficit in animal with deafferented cochlea [17] and hyperacusis in Fragile X mouse [18].

Then, the next question is if K_v3 modulators exert any unwanted effect on other K_v3 expressing neurons including the ones in the auditory end organ. Multiple K_v3 subtypes have been found in the cochlear nerve fibers [19, 20] and therefore, it is likely that K_v3 modulators affect the neuronal excitability in the cochlea. There are 4 major groups of nerve fibers in the sound sensing area of the cochlea. Type 1 afferent, which comprise ~90~95% of cochlear afferent nerve fibers, typically make single synaptic contact with single inner hair cell (IHC) [21]. Type 2 afferent, on the other hand, receives synaptic inputs from multiple outer hair cells (OHCs) [21, 22]. Efferent nerve fibers originated from the lateral olivary complex of the brainstem (LOC efferent) contact the most distal segment of the type 1 afferents and are thought to modulate the IHC-type 1 afferent synaptic transmission [23, 24]. Another group of efferent nerve fiber contacting the OHCs are originated from the medial olivary complex (MOC efferent) and regulate the sensitivity of sound detection system [23]. Until now, most studies provided only limited amount of information on K_v3 subtypes in cochlear afferents [19, 20, 25, 26] and efferent neuronal somas in the brainstem [6, 7, 27]. The subtype and subcellular localization of K_v3 channels in each neuronal component and their precise role at the hair cell synaptic transmission are yet to be discovered. The ultimate goal is to identify the precise localization of all K_v3 family K^+ channels within the cochlea and thereby, help assessing a therapeutic potential and adverse effect of K_v3 modulators. Here, we will focus on a subset of K_v3, namely $K_v3.1b$, $K_v3.3$, and $K_v3.4$, since their possible role in cochlear synaptic transmission has been anticipated from electrophysiological studies [26, 28-31].

MATERIALS AND METHODS

Sprague Dawley rats (4 to 9 weeks old, either sex) were used. Ultimate aim of this study was to identify K^+ channel subunit expression in cochlear nerve fibers of fully developed rat. At first, cochleas of 8~9-week-old rats were examined. Then, we increased our dataset by using cochlear tissues from 4~5-week-old rats. Our decision to do so can be justified because cochlear hair cell innervation pattern has already reached the adult form by the 4th postnatal week in rats and mice [32, 33]. Indeed, we did not notice any difference in the expression of various neural markers and K^+ channel subunits between 4~5-week vs 8~9-week-old rats. In cochleas of young rats and mice the fundamental properties of cochlear hair cell synaptic transmission did not exhibit any significant sex difference [34, 35]. Again, we did not notice any qualitative sex difference in a few cases where the sex of experimental subject was identified before the euthanasia. Therefore, we pooled the results from all ages and sex groups together. All procedures were performed in accordance with the animal protocol approved by the Mokpo National University Animal Care and Use Committee. Animals were euthanized by sevoflurane overdose and cochlear tissues were isolated for experiments. Tissue fixation and subsequent immunolabeling procedures were adapted from the methods previously described [36, 37]. The cochlea was perfused with 4% ice cold paraformaldehyde prepared in PBS (pH 7.4) through oval or round window and then fixed for 1 hour at 4°C. After 3 brief rinses with PBS the cochlear coil was carefully excised and immersed into a blocking/permeabilizing buffer (PBS supplemented with 5% donkey serum and 0.25% Triton-X 100) for 1 hour at room temperature. Then, the sample was incubated with primary antibodies diluted in the blocking/permeabilizing buffer at 4°C for 20 hour. Next day, the tissue was washed 3 times (each for 20 minutes) with the blocking/permeabilizing buffer. Fluorescence-labeled secondary antibodies diluted in blocking/permeabilizing buffer were incubated with the sample for 1 hour at room temperature. Then, the sample was rinsed once with blocking buffer for 20 minutes and twice with PBS for 10 minutes each. The tissue was mounted on a slide glass using FluorSave® mounting medium (Calbiochem, 345789). High-resolution images were obtained using a confocal laser scanning microscope (ZEISS, LMS 710). Confocal z-stacks were collected at 0.3~0.99 μm interval. Image analyses and reconstructions were carried out using image viewing software provided by the microscope manufacturers (Zeiss Zen), Imaris (version 7.3.0, Bitplane, Switzerland) and ImageJ (NIH). No labeling was observed when the primary antibodies were omitted. The list of primary antibodies is provided in Table 1. Donkey anti-chicken secondary antibody conjugated with Alexa Fluor 647 was purchased from Millipore (AP194SA6, 1:1,000). All other secondary antibodies (conjugated with Alexa Fluor 488, 555 or 633, generated in donkey) were purchased from Molecular Probes/Invitrogen and used at 1:1,000.

Table 1. Primary antibodies used in this study

Antigen	Host	Supplier	Catalog #	Dilution
$K_v3.1b$	Mouse monoclonal	Neuromab	75-041	1:500
$K_v3.3$	Mouse monoclonal	Neuromab	73-354	1:50
$K_v3.4$	Mouse monoclonal	Neuromab	75-112	1:500
Parvalbumin	Goat polyclonal	Swant	PVG-213	1:250
Calretinin	Rabbit polyclonal	Millipore	AB5054	1:500
Peripherin	Rabbit polyclonal	Millipore	AB1530	1:1,000
Choline acetyltransferase	Goat polyclonal	Millipore	AB144P	1:100
Na^+, K^+- ATPase α3	Rabbit polyclonal	NOVUS	NBP2-37955	1:500
Na^+, K^+- ATPase α3	Goat polyclonal	Santa Cruz Biotechnology	sc-16052	1:500
Caspr-2	Rabbit polyclonal	US Biological	C7865-2	1:500
Neurofilament H	Chicken polyclonal	Abcam	AB4680	1:1,000

RESULTS

$K_v3.1b$

$K_v3.1$ has 2 different splice variants, $K_v3.1a$ and $K_v3.1b$. $K_v3.1b$ appeared to be the primary isoform found in adult auditory neurons [38]. Expression of $K_v3.1b$ isoform in the soma of cochlear afferent nerve fibers (also known as spiral ganglion neurons (SGN)) and the contribution to neuronal firing is also well established [28]. However, it is unclear whether $K_v3.1b$ also modulates the excitatory postsynaptic potentials (EPSPs) at the IHC-type 1 afferent synaptic junction or participate only in the transmittance of action potential (AP) once large EPSP evokes AP at the heminode, the AP generation zone of type 1 afferent (corresponding to the fiber region penetrating habenular perforata in Fig. 1 diagram). Electrophysiological recording from the dendritic terminal of type 1 afferent suggested an existence of high-voltage-activating K^+ current at the IHC-type 1 afferent synaptic junction [36]. In contrast, previous immunolabeling studies reported $K_v3.1b$ signal at the heminode and the node of Ranvier [25, 26, 39] but not at the synaptic junction. To resolve this discrepancy, we closely examined the unmyelinated dendritic segments in addition to the cell body and the myelinated segment of the type 1 afferent. First, we compared $K_v3.1b$ signal with that of Na^+, K^+ ATPase α3 (NKA), a cellular marker for the type 1 afferent and MOC efferent nerve fibers [40]. Fig. 1A shows $K_v3.1b$ signal at the NKA-positive SGNs and nerve endings near IHCs. Higher magnification images of cell bodies (Fig.1B) and the distal segments (Fig. 1C) of the type 1 afferent fibers indicate that $K_v3.1b$ is present at the cell body as well as the most distal segment, the presumed heminode and node of Ranvier of NKA-positive fiber.

Co-labeling of $K_v3.1b$ and calretinin further confirmed that $K_v3.1b$ is expressed at the IHC-type 1 afferent synaptic junction. Calretinin is a cytosolic Ca^{2+} binding protein found in the hair cells and a subset of type 1 afferent fibers [37]. $K_v3.1b$ signal is found at the calretinin-positive dendritic terminals (Fig. 2A, yellow arrow) where they contact the calretinin-positive IHC. We also found some calretinin-negative but $K_v3.1b$-positive dendritic endings (Fig. 2A, white arrow) and cell bodies (Fig. 2B white arrow). In fact, type 1 afferent fibers, regardless of their calretinin content or the anatomical location of their synaptic junctions, appeared to express $K_v3.1b$ at their endings. Previous findings by us as well as by others consistently proposed that the absence of calretinin is one of the important cellular markers differentiating cochlear afferent fibers with low spontaneous firing rate, high-threshold to sound stimuli, and higher vulnerability to trauma [37, 41, 42]. Here, we hoped to find out whether there is a similar subgroup-specificity in the expression of $K_v3.1b$, a K^+ channel well known for regulating firing property of a neuron. However, $K_v3.1b$ signal was present in all NKA-positive SGNs, suggesting that $K_v3.1b$ essential component for type 1 cochlear afferents regardless of their sensitivity to sound or traumatic noise. Yet, one can speculate that the calretinin content might affect $K_v3.1b$ activity to some degree via intracellular Ca^{2+}-involved signaling cascade. For example, the physiologic characteristics of $K_v3.1b$ are known to be modulated by phosphorylation at a Ser residue of its cytoplasmic C-terminal domain [2]. Lower Ca^{2+} buffering capacity in calretinin-negative neurons might result in longer intracellular Ca^{2+} transient during neuronal activation, and higher chance of Ca^{2+}-dependent isoform of PKC activation, leading to $K_v3.1b$ phosphorylation and ultimately suppression of $K_v3.1b$ conductance.

Triple immunolabeling of $K_v3.1b$, NKA and Caspr-2 (the marker for node of Ranvier) demonstrated the $K_v3.1b$-hotspots at the heminode (Fig. 2C) and nodes of Ranvier (Fig. 2D) of NKA-positive fibers. $K_v3.1b$ is a high-voltage-activating K^+ channel with rapid activation and deactivation kinetics. Such kinetic property of $K_v3.1b$ would significantly speed up the AP repolarization phase while keeping the relative refractory period minimal. Therefore, we speculate that the $K_v3.1b$ at the heminodes and nodes of Ran-

https://doi.org/10.5607/en20043

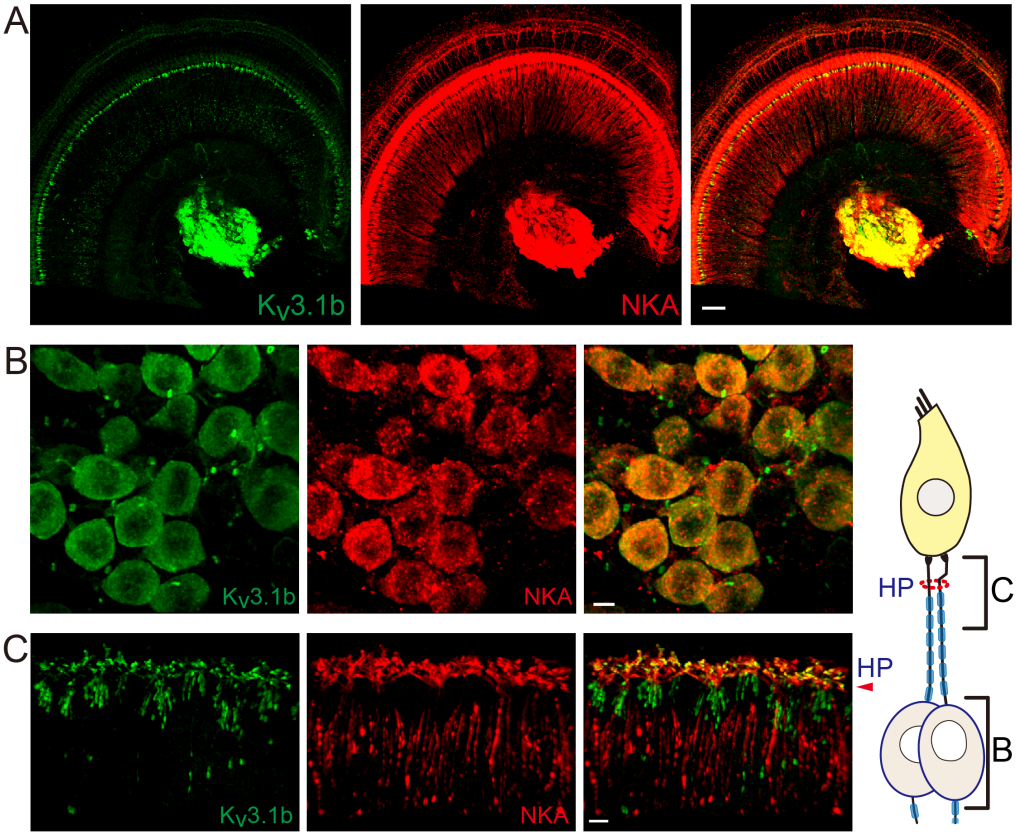

Fig. 1. $K_v3.1b$ is expressed in the type 1 afferents. (A) Low magnification images (n=2 cochlear preparations from 2 rats) of a cochlear preparation double-immunolabeled with anti-$K_v3.1b$ and anti-Na^+, K^+ ATPase α3 (NKA). Scale bar: 50 μm. (B, C) High magnification images of cell bodies (B, n=4 cochlear preparations from 3 rats) and peripheral processes (C, n=7 cochlear preparations from 4 rats) of type 1 afferents. $K_v3.1b$ signal is present in most NKA-positive cell bodies (100%, 214 out of 214 NKA-positive SGNs) and unmyelinated dendritic segments. The relative anatomical regions corresponding to each panel B and C are described in the diagram. HP: habenula perforata. Scale bar: 5 μm.

vier of cochlear afferents would contribute to generating and transmitting very brief APs at high rate along the cochlear afferent nerve fibers once suprathreshold synaptic potentials are evoked at the dendritic segment. Together, these results suggest that $K_v3.1b$ modulate IHC-driven synaptic potentials as well as subsequent AP transmittance along the type 1 afferent fibers.

$K_v3.3$

$K_v3.3$ is a high-voltage-activating K^+ channel with N-type inactivation mechanism [2]. Expression of $K_v3.3$ in mouse SGN soma has been previously demonstrated by immunostaining and mRNA analysis [19]. In many auditory brainstem neurons $K_v3.1b$ and $K_v3.3$ are often co-expressed and co-contribute to high frequency AP firing with minimal latency [6, 27]. Thus, we investigated whether $K_v3.3$ exhibited similar expression pattern as $K_v3.1b$ or was present in a distinctive group of nerve fibers. Double-immunolabeling of $K_v3.3$ and NKA revealed a weak $K_v3.3$ signal at the unmyelinated dendritic segments (Fig. 3A) and cell bodies of NKA-positive type 1 afferent fibers. Unlike $K_v3.1b$, we did not detect any $K_v3.3$ signal at the heminode or node of Ranvier of type 1 afferent. $K_v3.3$ signal at the spiral ganglion area largely overlapped with parvalbumin and NFH signals (Fig. 3B), indicating $K_v3.3$ expression in the soma of most type 1 afferent. In contrast, none of the peripherin-positive neurons showed $K_v3.3$ signal (Fig. 3C). Therefore, we concluded that $K_v3.3$ is expressed at the unmyelinated dendritic segment and cell body of type 1 but not type 2 afferent.

$K_v3.4$

$K_v3.4$, the last member of K_v3 family, has a high-voltage-activating and N-type inactivating property [2]. The presence of $K_v3.4$ immunoreactivity has been reported in guinea pig SGNs [20]. However, a more thorough examination was necessary because electrophysiological evidence from rat SGN suggested $K_v3.4$ expression in type 2 but not type 1 afferent fibers [30]. Initial immunolabeling data with anti-$K_v3.4$ revealed 3 different types of nerve fiber-like structures in the organ of Corti (Fig. 4); radial fibers projecting towards OHCs, spiral fibers near IHC, and spiral fibers near OHC. The shape and trajectory of the first and the second groups of $K_v3.4$-positive fibers are reminiscent of MOC and LOC efferent fibers, respectively. Because both MOC and LOC efferent fibers are predominantly cholinergic [23] we tested whether the $K_v3.4$-positive structures expressed choline acetyltransferase (ChAT). At the same time, we compared $K_v3.4$ signal with NKA-positive type 1 afferent and MOC efferent fibers [40]. The $K_v3.4$-positive radial fibers near OHCs had bouton-like endings contacting the OHC

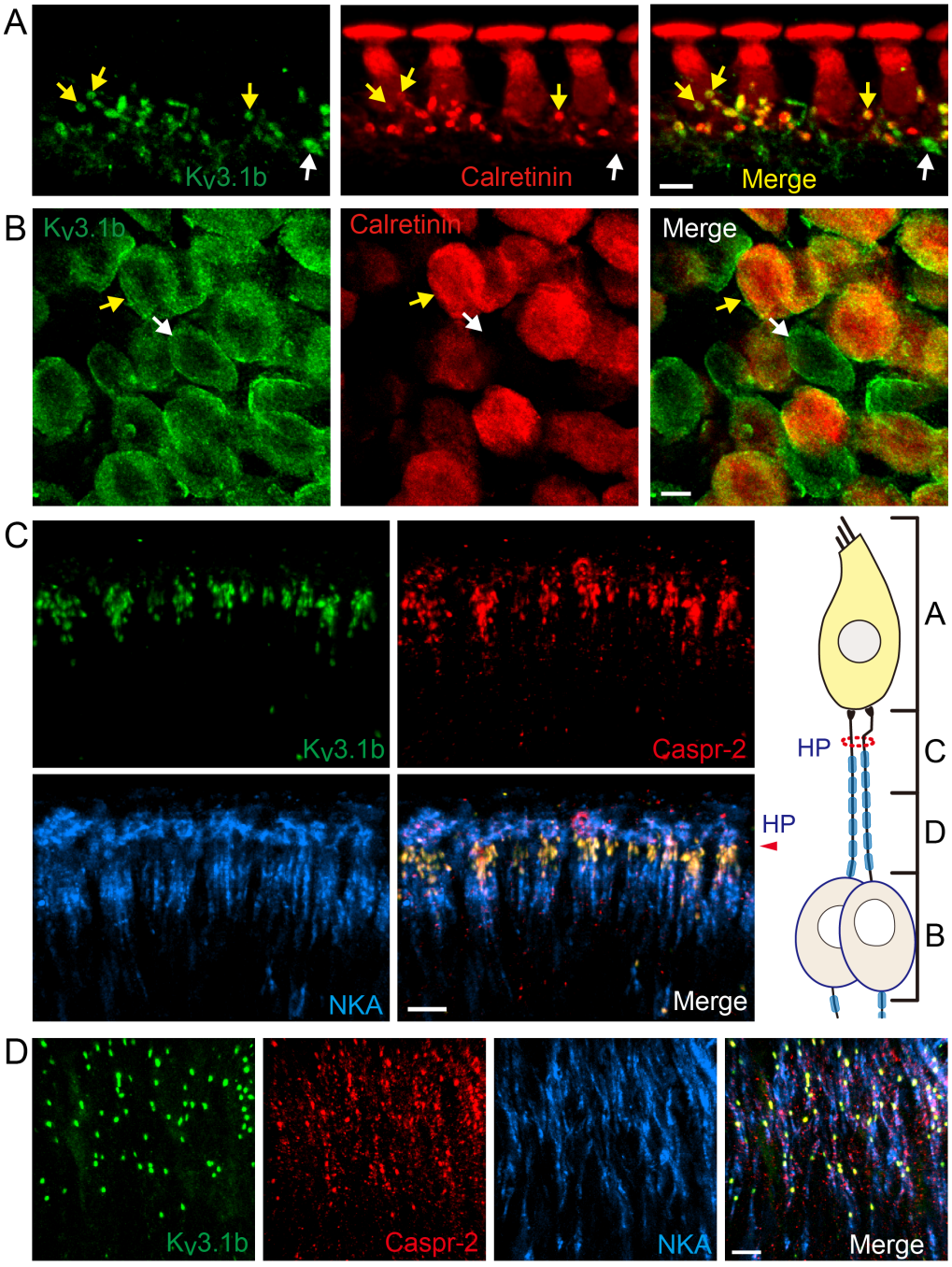

Fig. 2. K_v3.1b is expressed in the unmyelinated dendritic segments and the nodes of Ranvier of the type 1 cochlear afferent nerve fibers. The relative anatomical regions corresponding to each panel A-D are described in the diagram. Scale bar: 10 μm. (A) IHC-type 1 afferent fiber synapses immunolabeled with anti-K_v3.1b and anti-calretinin (n=6 cochlear preparations from 4 rats). K_v3.1b signal is found at the cochlear afferent fibers' dendritic terminals (yellow arrow) where they contact the IHCs. K_v3.1b-postive but calretinin-negative dendritic terminal (white arrow) is also found. (B) Spiral ganglion neurons (SGNs) immunolabeled with anti-K_v3.1b and anti-calretinin (n=4 cochlear preparations from 4 rats). K_v3.1b signal is found in both calretinin-positive (yellow arrow) and calretinin-negative (white arrow) neurons. Calretinin signal is present in 62.2% of K_v3.1b-positive SGNs (305 out of 490 K_v3.1b-positive SGNs). (C, D) Type 1 afferents immunolabeled with anti-K_v3.1b, anti-Caspr-2, and anti-NKA (n=6 cochlear preparations from 3 rats). K_v3.1b-hot spots along the nerve fiber correspond well with Caspr-2-signal.

base, and expressed both NKA and ChAT (Fig. 5A), indicating that the first group of fibers are indeed MOC efferent. In the area near IHCs, the K_v3.4-positive spiral fibers only crossed the NKA-positive fibers (Fig. 5B) and exhibited ChAT-signal (Fig. 5C), suggesting that this group of K_v3.4-positive fibers are LOC efferent.

The third group of K_v3.4-positive fibers expressed neither NKA nor ChAT. Based on their spiral trajectory near OHCs, we speculated them to be type 2 afferent. Because cell bodies and the peripheral processes of type 2 afferent fibers are known to express peripherin [43, 44] co-labeling of K_v3.4 with peripherin was performed. As expected, K_v3.4-positive neurons in spiral ganglion were NKA-negative (Fig. 6A) but peripherin-positive (Fig. 6B). Also, the K_v3.4 and peripherin signals co-localized in the spiral fibers near OHCs (Fig. 6C), indicating that this group of fibers are type 2 afferent.

https://doi.org/10.5607/en20043

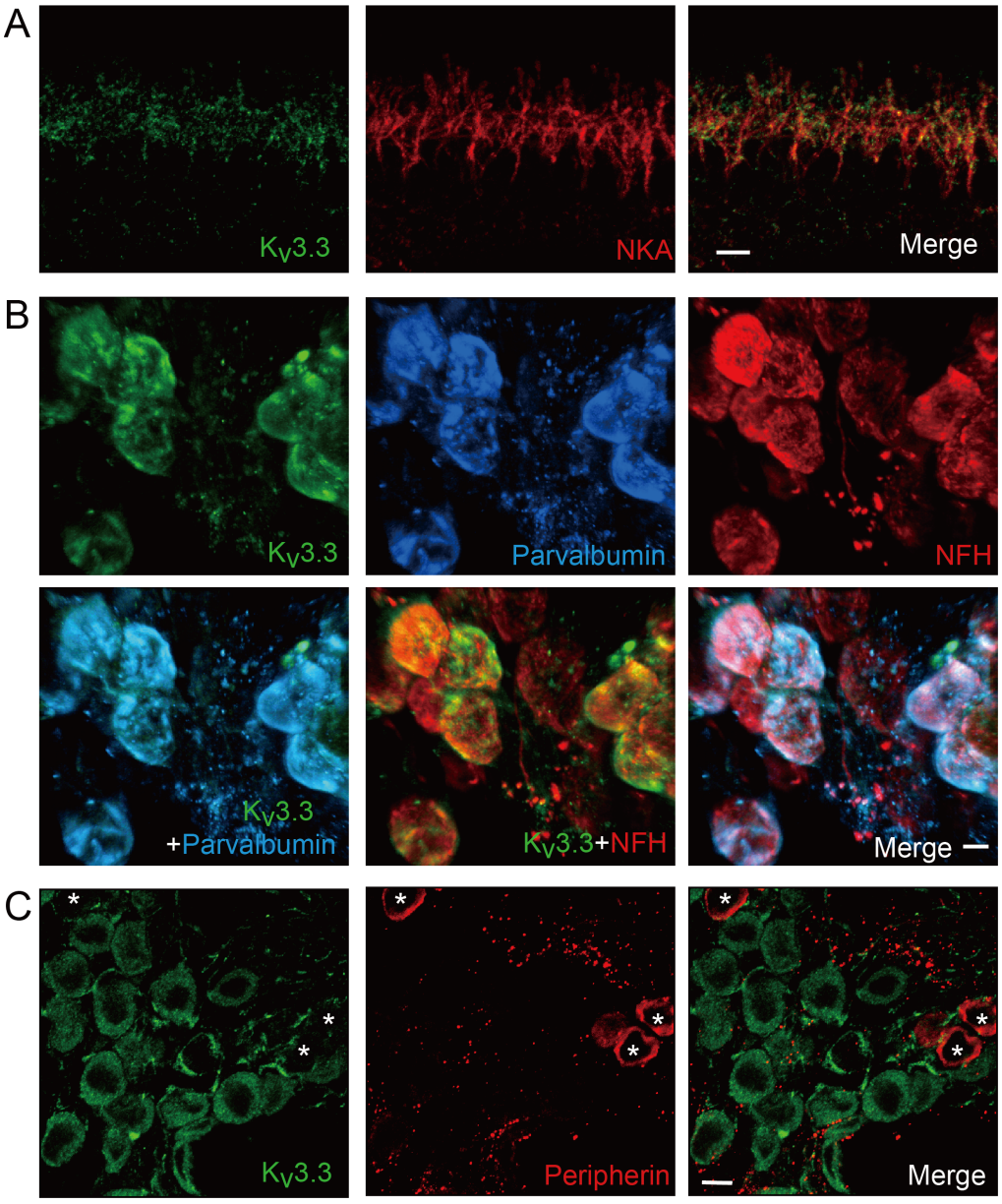

Fig. 3. $K_v3.3$ is expressed in type 1 but not in type 2 cochlear afferent nerve fibers. Scale bar: 5 μm. (A) The unmyelinated dendritic segments of cochlear afferent nerve fibers near IHC (n=3 cochlear preparations from 2 rats). The tissue was double-immunolabeled with anti-$K_v3.3$ and anti-NKA. Projection images were reconstructed from a partial z stack, covering only the depth of the unmyelinated dendritic segment of type 1 afferents. (B) SGNs immunolabeled with anti-$K_v3.3$, anti-parvalbumin, and anti-neurofilament H (NFH) (n=3 cochlear preparations from 2 rats). $K_v3.3$ signal was found in many parvalbumin- and NFH-positive neurons (64.7%, 22 out of 34 NFH-positive SGNs). (C) SGNs immunolabeled with anti-$K_v3.3$ and anti-peripherin (n=3 cochlear preparations from 2 rats). $K_v3.3$ is not expressed in peripherin-positive neurons (*).

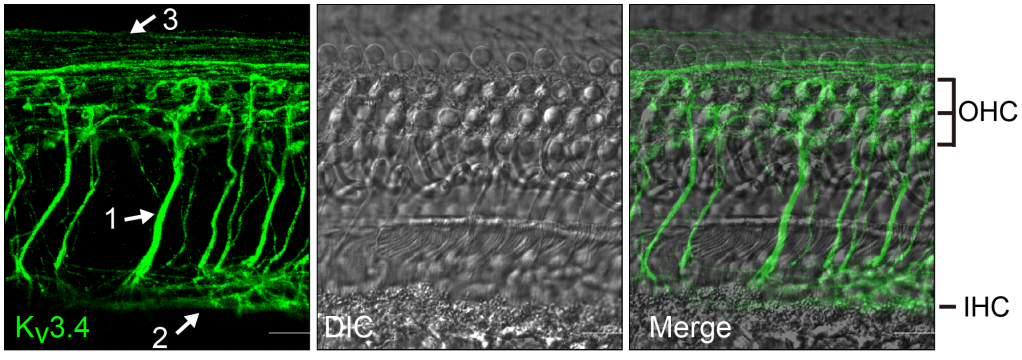

Fig. 4. $K_v3.4$ is expressed in 3 different types of nerve fibers in the organ of Corti. The tissue was immunolabeled with anti-$K_v3.4$ (n=10 cochlear preparations from 9 rats). $K_v3.4$ signal was found in radial fibers (1) projecting towards outer hair cells (OHC), spiral fibers traveling the basal pole of IHCs (2) and spiral fibers traveling near OHCs (3). Scale bar: 10 μm.

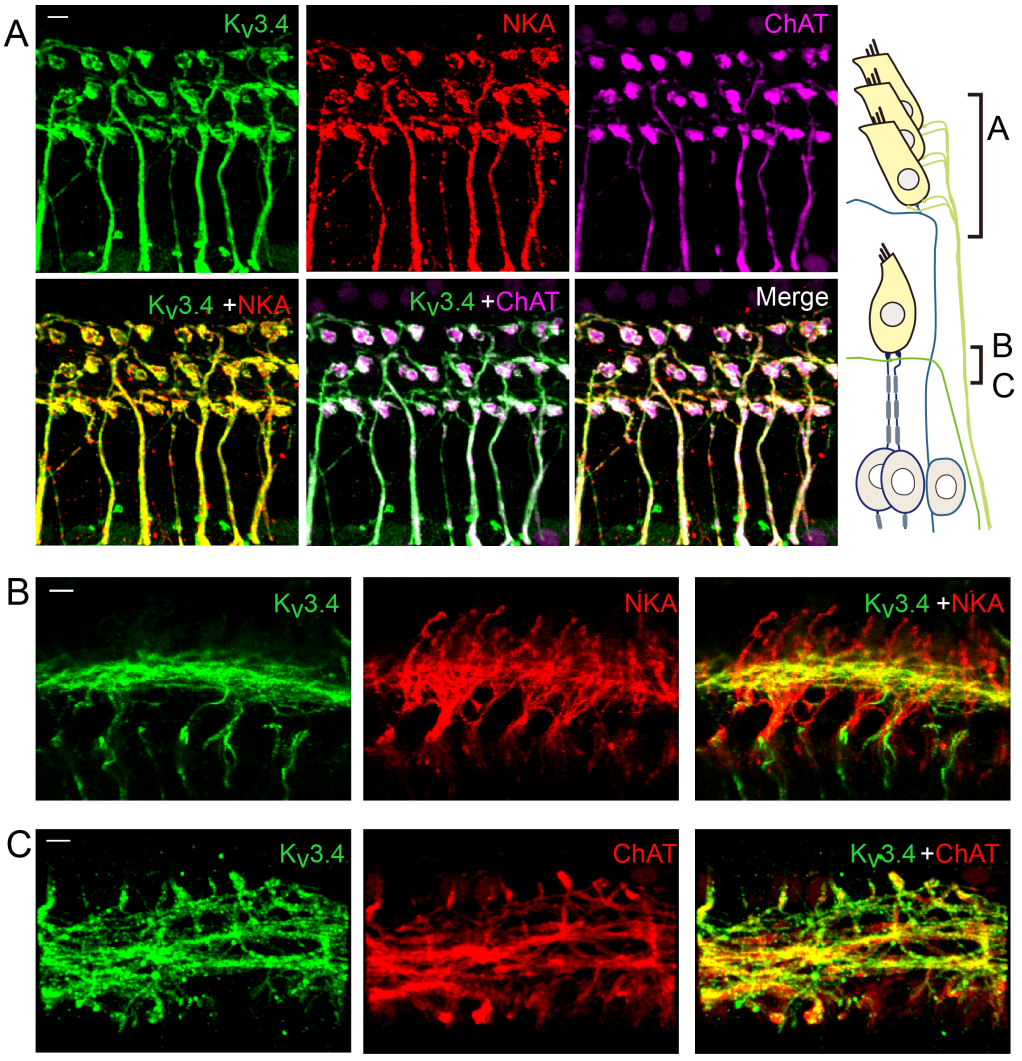

Fig. 5. $K_v3.4$ is expressed in choline acetyltransferase (ChAT)-positive cochlear efferent nerve fibers. Scale bar: 10 μm. (A) $K_v3.4$-positive radial fibers contacting OHCs are also positive for NKA and ChAT (2 cochlear preparations from 2 rats). (B) $K_v3.4$-positive spiral fibers near IHCs are ChAT-positive (C, 2 cochlear preparations from 2 rats) but NKA-negative (B, n=7 cochlear preparations from 7 rats). The relative anatomical regions corresponding to panel A-C are described in the diagram.

DISCUSSION

$K_v3.1b$ and $K_v3.3$ in auditory neurons

Coexpression of $K_v3.1b$ and $K_v3.3$ had been observed in several central auditory neurons [6, 45]. Similarly, gene analysis studies by others as well as our immunolabeling data consistently show that type 1 afferent in the cochlea, the first auditory neuron in the ascending pathway, co-express $K_v3.1b$ and $K_v3.3$. Quantitative RT-PCR of cultured mouse SGNs found mRNAs for $K_v3.1$ and $K_v3.3$ [19]. More recent studies using single cell RNA seq or RNAscope techniques reported $K_v3.1$ and $K_v3.3$ genes in type 1 but not in type 2 mouse SGN [41, 46]. Here, we found $K_v3.1b$ and $K_v3.3$-immunoreactivities in type 1 but not type 2 SGNs. $K_v3.1b$ and $K_v3.3$ are both high-voltage-activating K^+ channels but have different inactivation properties. $K_v3.1b$ shows only slight inactivation at positive potentials while $K_v3.3$ inactivates upon prolonged depolarization to +10 mV or more positive [2]. Electrophysiological recordings of auditory brainstem neurons indicated that both $K_v3.1b$ and $K_v3.3$ facilitate high frequency repetitive firing [8, 27] and different K_v3 subunits in same neuron appeared to exert compensatory role although the relative contribution in different sets of neurons might vary. For example, $K_v3.3$ has dominant role in LSO neurons while both $K_v3.1b$ and $K_v3.3$ contribute in MNTB neurons [27]. In type 1 afferents, it is still unclear whether $K_v3.1b$ and $K_v3.3$ contribute equally to the high frequency firing or not. Patch clamp recordings of cultured mouse SGN have reported that dendrotoxin (selective K_v1 inhibitor; [47])-resistant high-voltage-activating K^+ current was non-inactivating type [26, 31], supporting dominant role of $K_v3.1b$ over $K_v3.3$. However, the amount of $K_v3.3$ mRNA was higher than that of $K_v3.1$ in freshly isolated mouse SGN [19]. Also, high-voltage-activating K^+ current recorded from freshly isolated neonatal rat SGNs revealed inactivating component [29]. Therefore, further investigation using freshly isolated mature SGN is necessary to determine the relative contribution of $K_v3.1b$ and

https://doi.org/10.5607/en20043

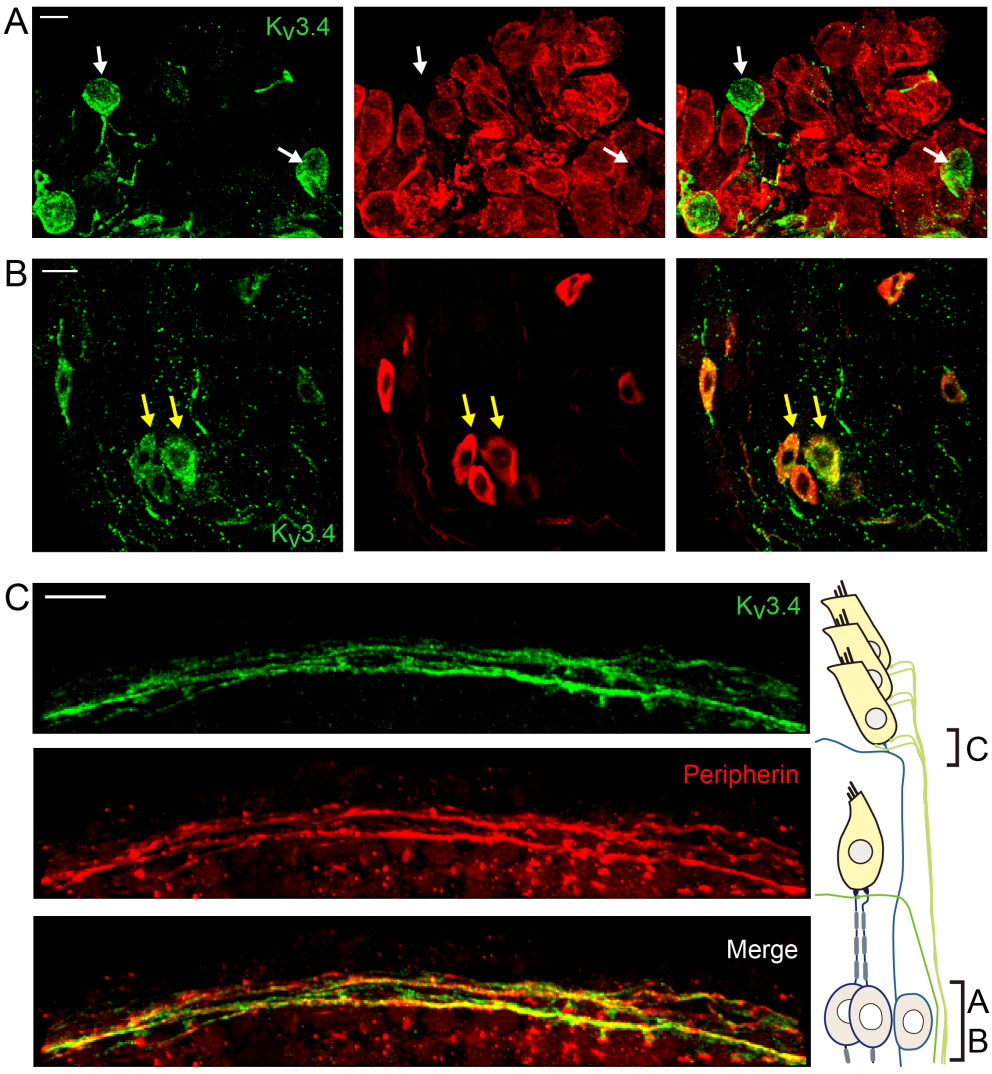

Fig. 6. K_v3.4 is expressed in type 2 cochlear afferent nerve fibers. Scale bar: 10 μm. (A) SGNs immunolabeled with anti-K_v3.4 and anti-NKA (n=6 cochlear preparations from 3 rats). K_v3.4 signal (white arrow) is not found in most NKA-positive neurons (weak K_v3.4 signal in only 2 out of 424 NKA-positive neurons). (B) SGNs immunolabeled with anti-K_v3.4 and anti-peripherin (n=5 cochlear preparations from 4 rats). K_v3.4 signal is found in peripherin-positive neurons (yellow arrow; 97.7%, 84 out of 86 peripherin-positive neurons). (C) K_v3.4-positive spiral fibers near OHCs (n=3 cochlear preparations from 3 rats). K_v3.4 signal largely overlaps with peripherin signal. The relative anatomical regions corresponding to panel A~C are described in the diagram.

K_v3.3 to the high-voltage-activating K^+ current in type 1 afferents.

Previous immunolabeling studies reported K_v3.1b signal at the heminode and the node of Ranvier [25, 26, 39] but not at the unmyelinated dendritic segment of type 1 afferent. In contrast, we consistently found K_v3.1b and K_v3.3 at the unmyelinated dendritic segments of type 1 afferent (Fig. 2A). Interestingly, studies on Na_v1.6 in type 1 afferent reported similar contradictory findings. Hossain and colleagues reported Na_v1.6 expression at unmyelinated dendritic segment as well as the heminode, nodes of Ranvier of type 1 afferent in mouse cochlea [48] while others reported Na_v1.6 signal at the heminode, nodes of Ranvier but not at the dendritic segment [25, 39]. Considering the observation of occasional stronger K_v3.1b signal at the heminode than at the dendritic segment in some cochlear tissues (Fig. 2A vs. 2C), we suspect that the discrepancy might be due to an underestimation of dendritic signal juxtaposing the relatively strong signal at the heminode.

Then, what is the physiological role of the high-voltage-activating ion channels at the dendrite, away from the AP initiation zone of type 1 afferent? The IHC-type 1 afferent synaptic junction is <50 μm away from the AP initiation zone [40, 49] and therefore, the membrane potential at the synaptic junction could easily reach the voltage range of K_v3 activation during synaptic events. Intracellular recording from the dendritic terminal of type 1 afferent confirmed that significant portion of IHC-driven EPSPs were large enough to generate APs (in P7-14 rat ~18% [36], in P17-19 rat 81~97% [49]). Furthermore, the voltage dependence and other biophysical properties of K_v3 are known to be modulated by multiple mechanisms [2]. For example, dephosphorylated K_v3.1b, compared to their phosphorylated counterpart, showed significantly more negative activation voltage ranges ($V_{1/2}$max -3.92 mV vs. 16.9 mV) and larger amplitude [50]. It implies that the impact of K_v3 on IHC-type 1 afferent synaptic transmission could get even more extensive

depending on the strength of various modulatory mechanisms.

K_v3.4 in type 2 afferent, MOC and LOC efferent

A presence of K_v3.4 in type 2 afferents had been initially predicted in a simultaneous patch clamp recording and dye-filling experiment on neonatal rat SGNs [30]. The OHC-innervating type 2 SGNs, compared to the IHC-contacting type 1 afferents, exhibited much more rapidly and prominently inactivating A type K^+ current. From the kinetic properties and voltage dependence, K_v3.4 has been proposed as one of the channels responsible for the A current in type 2 SGNs. A later immunolabeling study suggested K_v3.4 expression in both type 1 and type 2 SGNs because 86~91% of guinea pig SGNs were K_v3.4-positive [20]. Recent gene analysis on mouse SGNs indicated K_v3.4 in type 2 but not in type 1 SGNs [41, 46]. In our immunolabeling result, only a small fraction of 4~9-week-old rat SGNs were K_v3.4-positive. Furthermore, K_v3.4 signal was found in peripherin-positive SGNs and nerve fibers near OHC but not in NKA-positive SGNs. Therefore, we conclude that K_v3.4 is specific for type 2 afferent at least in rats and mice.

Additionally, we found K_v3.4 in MOC and LOC efferent fiber axons in the organ of Corti. Both branches of efferent systems are known to provide cochlear protection upon noise exposure. MOC efferent fibers, by regulating electromotility of OHCs, modulate the sensitivity of 'cochlear amplifier' and prevent hair cell damage upon noise exposure [51-53]. Similarly, LOC efferent fibers, at least in part by modulating glutamate release from IHC, protect type 1 afferents from excitotoxic damage [24, 54]. Not surprisingly, neurotransmitter release from cochlear efferent fiber axons are modulated by multiple mechanisms [55, 56]. Metabotropic glutamate receptor, voltage gated Ca^{2+} channels and Ca^{2+}-activated BK K^+ channel at the presynaptic efferent fiber axons had been reported to contribute to the efferent synaptic transmission [56-58]. Here, based on our finding of K_v3.4 at the MOC and LOC efferent fiber axons, we propose to add K_v3.4 to the list of proteins modulating cochlear efferent neurotransmitter release. Currently available electrophysiological evidence from MOC and LOC neurons also do not reject this possibility. Patch clamp recordings from LOC neurons in mouse brain slices exhibited prominent A type current [59]. In another study MOC and LOC neurons were recorded after retrograde labeling by dye injection to the rat cochlea and both labeled MOC and LOC neurons displayed A type K^+ current although the kinetic properties, voltage dependence, and relative sensitivity to a K^+ channel inhibitor 4-AP differed somewhat [60]. Indeed, contribution of K_v3.4 to synaptic release has been demonstrated in other peripheral and central neurons. For example, in dorsal root ganglion nociceptors, K_v3.4 has been shown to participate in AP repolarization at the presynaptic axon terminal and consequently to modulate pain synaptic transmission [61-63]. In cerebellar stellate cells, the availability and state of K_v3.4 at synaptic boutons could be rapidly altered by the prior activity history of the neuron, which enabled rapid modulation of AP waveform at the synaptic boutons and ultimately provided flexibility to the synaptic transmission [64]. Beside the rapid voltage-dependent inactivation, K_v3.4 can also be switched from rapidly inactivating A type to non-inactivating type by modification on the N-terminal inactivation domain [2, 61]. It suggests that the prior activity history of each K_v3.4-expressing nerve fiber might modulate the status of K_v3.4 differently and therefore, provide another layer of fine tuning to neurotransmitter release.

To summarize, we have demonstrated that K_v3.1b and K_v3.3 are expressed in type 1 afferent and K_v3.4 in type 2 and efferent cochlear nerve fibers. These findings suggest that different K_v3 subtypes are likely assigned for different auditory tasks, for example, K_v3.1b and K_v3.3 in ascending signaling while K_v3.4 in protective feedback upon loud noise exposure. The data also indicates that K_v3 modulators, depending on the spectrum of action, might affect the neuronal excitability of different sets of the cochlear nerve fibers and modify different aspects of auditory processing in the cochlea.

ACKNOWLEDGEMENTS

Authors appreciate late Dr. Young-Woo Seo of Korea Basic Science Institute Gwangju Center for his technical support and critical comments during the early stage of this work.

AUTHOR CONTRIBUTIONS

WBK, K-WK, and KS performed the experiments and analyzed the data. WBK and EY wrote the manuscript. EY supervised the project.

FUNDING

This work was supported by Basic Science Research Program through the National Research Foundation of Korea (NRF) funded by the Ministry of Education (2019R1I1A3A01063625 to EY).

REFERENCES

1. Rudy B, McBain CJ (2001) Kv3 channels: voltage-gated K+ channels designed for high-frequency repetitive firing. Trends Neurosci 24:517-526.
2. Kaczmarek LK, Zhang Y (2017) Kv3 channels: enablers of

rapid firing, neurotransmitter release, and neuronal endurance. Physiol Rev 97:1431-1468.
3. Trussell LO (1997) Cellular mechanisms for preservation of timing in central auditory pathways. Curr Opin Neurobiol 7:487-492.
4. Spirou GA, Brownell WE, Zidanic M (1990) Recordings from cat trapezoid body and HRP labeling of globular bushy cell axons. J Neurophysiol 63:1169-1190.
5. Smith PH, Joris PX, Carney LH, Yin TC (1991) Projections of physiologically characterized globular bushy cell axons from the cochlear nucleus of the cat. J Comp Neurol 304:387-407.
6. Li W, Kaczmarek LK, Perney TM (2001) Localization of two high-threshold potassium channel subunits in the rat central auditory system. J Comp Neurol 437:196-218.
7. Nabel AL, Callan AR, Gleiss SA, Kladisios N, Leibold C, Felmy F (2019) Distinct distribution patterns of potassium channel sub-units in somato-dendritic compartments of neurons of the medial superior olive. Front Cell Neurosci 13:38.
8. Wang LY, Gan L, Forsythe ID, Kaczmarek LK (1998) Contribution of the Kv3.1 potassium channel to high-frequency firing in mouse auditory neurones. J Physiol 509(Pt 1)(Pt 1):183-194.
9. Olsen T, Capurro A, Pilati N, Large CH, Hamann M (2018) Kv3 K+ currents contribute to spike-timing in dorsal cochlear nucleus principal cells. Neuropharmacology 133:319-333.
10. Macica CM, von Hehn CA, Wang LY, Ho CS, Yokoyama S, Joho RH, Kaczmarek LK (2003) Modulation of the kv3.1b potassium channel isoform adjusts the fidelity of the firing pattern of auditory neurons. J Neurosci 23:1133-1141.
11. Ho CS, Grange RW, Joho RH (1997) Pleiotropic effects of a disrupted K+ channel gene: reduced body weight, impaired motor skill and muscle contraction, but no seizures. Proc Natl Acad Sci U S A 94:1533-1538.
12. Kaltenbach JA, Rachel JD, Mathog TA, Zhang J, Falzarano PR, Lewandowski M (2002) Cisplatin-induced hyperactivity in the dorsal cochlear nucleus and its relation to outer hair cell loss: relevance to tinnitus. J Neurophysiol 88:699-714.
13. Kalappa BI, Brozoski TJ, Turner JG, Caspary DM (2014) Single unit hyperactivity and bursting in the auditory thalamus of awake rats directly correlates with behavioural evidence of tinnitus. J Physiol 592:5065-5078.
14. Ma WL, Hidaka H, May BJ (2006) Spontaneous activity in the inferior colliculus of CBA/J mice after manipulations that induce tinnitus. Hear Res 212:9-21.
15. Anderson LA, Hesse LL, Pilati N, Bakay WMH, Alvaro G, Large CH, McAlpine D, Schaette R, Linden JF (2018) Increased spontaneous firing rates in auditory midbrain following noise exposure are specifically abolished by a Kv3 channel modulator. Hear Res 365:77-89.
16. Glait L, Fan W, Stillitano G, Sandridge S, Pilati N, Large C, Alvaro G, Kaltenbach JA (2018) Effects of AUT00063, a Kv3.1 channel modulator, on noise-induced hyperactivity in the dorsal cochlear nucleus. Hear Res 361:36-44.
17. Chambers AR, Pilati N, Balaram P, Large CH, Kaczmarek LK, Polley DB (2017) Pharmacological modulation of Kv3.1 mitigates auditory midbrain temporal processing deficits following auditory nerve damage. Sci Rep 7:17496.
18. El-Hassar L, Song L, Tan WJT, Large CH, Alvaro G, Santos-Sacchi J, Kaczmarek LK (2019) Modulators of Kv3 potassium channels rescue the auditory function of fragile X mice. J Neurosci 39:4797-4813.
19. Chen WC, Davis RL (2006) Voltage-gated and two-pore-domain potassium channels in murine spiral ganglion neurons. Hear Res 222:89-99.
20. Bakondi G, Pór A, Kovács I, Szucs G, Rusznák Z (2008) Voltage-gated K+ channel (Kv) subunit expression of the guinea pig spiral ganglion cells studied in a newly developed cochlear free-floating preparation. Brain Res 1210:148-162.
21. Berglund AM, Ryugo DK (1987) Hair cell innervation by spiral ganglion neurons in the mouse. J Comp Neurol 255:560-570.
22. Weisz CJ, Glowatzki E, Fuchs PA (2014) Excitability of type II cochlear afferents. J Neurosci 34:2365-2373.
23. Guinan JJ Jr (2018) Olivocochlear efferents: their action, effects, measurement and uses, and the impact of the new conception of cochlear mechanical responses. Hear Res 362:38-47.
24. Wu JS, Yi E, Manca M, Javaid H, Lauer AM, Glowatzki E (2020) Sound exposure dynamically induces dopamine synthesis in cholinergic LOC efferents for feedback to auditory nerve fibers. Elife 9:e52419.
25. Kim KX, Rutherford MA (2016) Maturation of NaV and KV channel topographies in the auditory nerve spike initiator before and after developmental onset of hearing function. J Neurosci 36:2111-2118.
26. Smith KE, Browne L, Selwood DL, McAlpine D, Jagger DJ (2015) Phosphoinositide modulation of heteromeric Kv1 channels adjusts output of spiral ganglion neurons from hearing mice. J Neurosci 35:11221-11232.
27. Choudhury N, Linley D, Richardson A, Anderson M, Robinson SW, Marra V, Ciampani V, Walter SM, Kopp-Scheinpflug C, Steinert JR, Forsythe ID (2020) Kv3.1 and Kv3.3 subunits differentially contribute to Kv3 channels and action potential repolarization in principal neurons of the auditory brainstem.

J Physiol 598:2199-2222.
28. Adamson CL, Reid MA, Mo ZL, Bowne-English J, Davis RL (2002) Firing features and potassium channel content of murine spiral ganglion neurons vary with cochlear location. J Comp Neurol 447:331-350.
29. Jagger DJ, Housley GD (2002) A-type potassium currents dominate repolarisation of neonatal rat primary auditory neurones in situ. Neuroscience 109:169-182.
30. Jagger DJ, Housley GD (2003) Membrane properties of type II spiral ganglion neurones identified in a neonatal rat cochlear slice. J Physiol 552(Pt 2):525-533.
31. Mo ZL, Adamson CL, Davis RL (2002) Dendrotoxin-sensitive K(+) currents contribute to accommodation in murine spiral ganglion neurons. J Physiol 542(Pt 3):763-778.
32. Wu JS, Young ED, Glowatzki E (2016) Maturation of spontaneous firing properties after hearing onset in rat auditory nerve fibers: spontaneous rates, refractoriness, and interfiber correlations. J Neurosci 36:10584-10597.
33. Liberman LD, Liberman MC (2016) Postnatal maturation of auditory-nerve heterogeneity, as seen in spatial gradients of synapse morphology in the inner hair cell area. Hear Res 339:12-22.
34. Rohmann KN, Wersinger E, Braude JP, Pyott SJ, Fuchs PA (2015) Activation of BK and SK channels by efferent synapses on outer hair cells in high-frequency regions of the rodent cochlea. J Neurosci 35:1821-1830.
35. Grant L, Yi E, Glowatzki E (2010) Two modes of release shape the postsynaptic response at the inner hair cell ribbon synapse. J Neurosci 30:4210-4220.
36. Yi E, Roux I, Glowatzki E (2010) Dendritic HCN channels shape excitatory postsynaptic potentials at the inner hair cell afferent synapse in the mammalian cochlea. J Neurophysiol 103:2532-2543.
37. Sharma K, Seo YW, Yi E (2018) Differential expression of Ca^{2+}-buffering protein calretinin in cochlear afferent fibers: a possible link to vulnerability to traumatic noise. Exp Neurobiol 27:397-407.
38. Perney TM, Marshall J, Martin KA, Hockfield S, Kaczmarek LK (1992) Expression of the mRNAs for the Kv3.1 potassium channel gene in the adult and developing rat brain. J Neurophysiol 68:756-766.
39. Reijntjes DOJ, Lee JH, Park S, Schubert NMA, van Tuinen M, Vijayakumar S, Jones TA, Jones SM, Gratton MA, Xia XM, Yamoah EN, Pyott SJ (2019) Sodium-activated potassium channels shape peripheral auditory function and activity of the primary auditory neurons in mice. Sci Rep 9:2573.
40. McLean WJ, Smith KA, Glowatzki E, Pyott SJ (2009) Distribution of the Na,K-ATPase alpha subunit in the rat spiral ganglion and organ of corti. J Assoc Res Otolaryngol 10:37-49.
41. Shrestha BR, Chia C, Wu L, Kujawa SG, Liberman MC, Goodrich LV (2018) Sensory neuron diversity in the inner ear is shaped by activity. Cell 174:1229-1246.e17.
42. Sun S, Babola T, Pregernig G, So KS, Nguyen M, Su SM, Palermo AT, Bergles DE, Burns JC, Müller U (2018) Hair cell mechanotransduction regulates spontaneous activity and spiral ganglion subtype specification in the auditory system. Cell 174:1247-1263.e15.
43. V Vyas P, Wu JS, Zimmerman A, Fuchs P, Glowatzki E (2017) Tyrosine hydroxylase expression in type II cochlear afferents in mice. J Assoc Res Otolaryngol 18:139-151.
44. Hafidi A (1998) Peripherin-like immunoreactivity in type II spiral ganglion cell body and projections. Brain Res 805:181-190.
45. Grigg JJ, Brew HM, Tempel BL (2000) Differential expression of voltage-gated potassium channel genes in auditory nuclei of the mouse brainstem. Hear Res 140:77-90.
46. Petitpré C, Wu H, Sharma A, Tokarska A, Fontanet P, Wang Y, Helmbacher F, Yackle K, Silberberg G, Hadjab S, Lallemend F (2018) Neuronal heterogeneity and stereotyped connectivity in the auditory afferent system. Nat Commun 9:3691.
47. Harvey AL, Robertson B (2004) Dendrotoxins: structure-activity relationships and effects on potassium ion channels. Curr Med Chem 11:3065-3072.
48. Hossain WA, Antic SD, Yang Y, Rasband MN, Morest DK (2005) Where is the spike generator of the cochlear nerve? Voltage-gated sodium channels in the mouse cochlea. J Neurosci 25:6857-6868.
49. Rutherford MA, Chapochnikov NM, Moser T (2012) Spike encoding of neurotransmitter release timing by spiral ganglion neurons of the cochlea. J Neurosci 32:4773-4789.
50. Macica CM, Kaczmarek LK (2001) Casein kinase 2 determines the voltage dependence of the Kv3.1 channel in auditory neurons and transfected cells. J Neurosci 21:1160-1168.
51. Guinan JJ Jr (2010) Cochlear efferent innervation and function. Curr Opin Otolaryngol Head Neck Surg 18:447-453.
52. Maison SF, Usubuchi H, Liberman MC (2013) Efferent feedback minimizes cochlear neuropathy from moderate noise exposure. J Neurosci 33:5542-5552.
53. Boero LE, Castagna VC, Di Guilmi MN, Goutman JD, Elgoyhen AB, Gómez-Casati ME (2018) Enhancement of the medial olivocochlear system prevents hidden hearing loss. J Neurosci 38:7440-7451.
54. Darrow KN, Maison SF, Liberman MC (2007) Selective re-

moval of lateral olivocochlear efferents increases vulnerability to acute acoustic injury. J Neurophysiol 97:1775-1785.
55. Goutman JD, Fuchs PA, Glowatzki E (2005) Facilitating efferent inhibition of inner hair cells in the cochlea of the neonatal rat. J Physiol 566(Pt 1):49-59.
56. Zorrilla de San Martín J, Pyott S, Ballestero J, Katz E (2010) Ca(2+) and Ca(2+)-activated K(+) channels that support and modulate transmitter release at the olivocochlear efferent-inner hair cell synapse. J Neurosci 30:12157-12167.
57. Ye Z, Goutman JD, Pyott SJ, Glowatzki E (2017) mGluR1 enhances efferent inhibition of inner hair cells in the developing rat cochlea. J Physiol 595:3483-3495.
58. Vattino LG, Wedemeyer C, Elgoyhen AB, Katz E (2020) Functional postnatal maturation of the medial olivocochlear efferent-outer hair cell synapse. J Neurosci 40:4842-4857.
59. Sterenborg JC, Pilati N, Sheridan CJ, Uchitel OD, Forsythe ID, Barnes-Davies M (2010) Lateral olivocochlear (LOC) neurons of the mouse LSO receive excitatory and inhibitory synaptic inputs with slower kinetics than LSO principal neurons. Hear Res 270:119-126.
60. Fujino K, Koyano K, Ohmori H (1997) Lateral and medial olivocochlear neurons have distinct electrophysiological properties in the rat brain slice. J Neurophysiol 77:2788-2804.
61. Ritter DM, Zemel BM, Lepore AC, Covarrubias M (2015) Kv3.4 channel function and dysfunction in nociceptors. Channels (Austin) 9:209-217.
62. Ritter DM, Zemel BM, Hala TJ, O'Leary ME, Lepore AC, Covarrubias M (2015) Dysregulation of Kv3.4 channels in dorsal root ganglia following spinal cord injury. J Neurosci 35:1260-1273.
63. Muqeem T, Ghosh B, Pinto V, Lepore AC, Covarrubias M (2018) Regulation of nociceptive glutamatergic signaling by presynaptic Kv3.4 channels in the rat spinal dorsal horn. J Neurosci 38:3729-3740.
64. Rowan MJM, Christie JM (2017) Rapid state-dependent alteration in Kv3 channel availability drives flexible synaptic signaling dependent on somatic subthreshold depolarization. Cell Rep 18:2018-2029.